

ON THE INEVITABILITY OF REIONIZATION:  
IMPLICATIONS FOR COSMIC MICROWAVE  
BACKGROUND FLUCTUATIONS<sup>1</sup>

Max Tegmark<sup>1</sup>, Joseph Silk<sup>2</sup> & Alain Blanchard<sup>3</sup>

<sup>1</sup>*Department of Physics, University of California, Berkeley, California 94720*

<sup>2</sup>*Departments of Astronomy and Physics, and Center for Particle Astrophysics,  
University of California, Berkeley, California 94720*

<sup>3</sup>*DAEC, Observatoire de Paris-Meudon, 92190 Meudon, France*

**Abstract**

Early photoionization of the intergalactic medium is discussed in a nearly model-independent way, in order to investigate whether early structures corresponding to rare Gaussian peaks in a CDM model can photoionize the intergalactic medium sufficiently early to appreciably smooth out the microwave background fluctuations. We conclude that this is indeed possible for a broad range of CDM normalizations and is almost inevitable for unbiased CDM, provided that the bulk of these early structures are quite small, no more massive than about  $10^8 M_\odot$ . Typical parameter values predict that reionization occurs around  $z = 50$ , thereby suppressing fluctuations on degree scales while leaving the larger angular scales probed by COBE reasonably unaffected. However, for non-standard CDM, incorporating mixed dark matter, vacuum density or a tilted primordial power spectrum, early reionization plays no significant role.

---

<sup>1</sup> Published in *ApJ*, **420**, 486, January 10, 1994.

Submitted March 18 1993, accepted July 2. Available from

<http://www.sns.ias.edu/~max/reion.html> (faster from the US) and from

<http://www.mpa-garching.mpg.de/~max/reion.html> (faster from Europe).

# 1 Introduction

The first quantitative predictions of cosmic microwave background anisotropies in cold dark matter (CDM)-dominated cosmological models recognized that reionization by rare, early-forming objects could play a role in suppressing temperature fluctuations on small angular scales (Bond & Efstathiou 1984; Vittorio & Silk 1984). Now that the COBE DMR experiment has detected fluctuations on large angular scales (Smoot *et al.* 1992) at a level (within a factor of two) comparable to that predicted by CDM models, it is especially relevant to examine whether reionization can affect the degree scale searches that are currently underway.

Cold dark matter models are generally characterized by a late epoch of galaxy formation. However, the smallest and oldest objects first go nonlinear at relatively large redshift. In this paper we investigate, for a wide range of CDM normalizations, power spectra and efficiency parameters, whether reionization associated with energy injection by early forming dwarf galaxies can reionize the universe sufficiently early to smooth out primordial CBR temperature fluctuations.

Although we go into some detail in the appendix to make estimates of a certain efficiency parameter, our overall treatment is fairly model-independent, and can be used as a framework within which to compare various photoionization scenarios. Our basic picture is roughly the following: An ever larger fraction of the baryons in the universe falls into nonlinear structures and forms galaxies. A certain fraction of these baryons form stars or quasars which emit ultraviolet radiation, and some of this radiation escapes into the ambient intergalactic medium (IGM) and ends up photoionizing and heating it. Due to cooling losses and recombinations, the net number of ionizations per UV photon is generally less than unity.

Apart from photoionization, early galaxies can also ionize the IGM through supernova driven winds, an ionization mechanism that will not be treated in this paper. Although such winds can ionize the IGM by  $z = 5$ , early enough to explain the absence of a Gunn-Peterson effect (Tegmark *et al.* 1993), the relatively low velocities of such winds makes them unable to distribute the released energy throughout space at redshifts early enough (by  $z \approx 50$ ) to measurably affect the CBR.

Our approach will be to first write the ionization fraction of the IGM as a product of a number of factors, and then discuss the value of each of these

factors in more detail. Let us write

$$\chi = f_s f_{uvpp} f_{ion}, \quad (1)$$

where

$$\begin{cases} \chi & = \text{fraction of IGM that is ionized,} \\ f_s & = \text{fraction of baryons in nonlinear structures,} \\ f_{uvpp} & = \text{UV photons emitted into IGM per proton in nonlinear structures,} \\ f_{ion} & = \text{net ionizations per emitted UV photon.} \end{cases}$$

Let us first consider the case where the UV photons are produced by stars, and return to the quasar case later. Using the fact that a fraction 0.0073 of the rest mass is released in stellar burning of hydrogen to helium, we obtain

$$f_{uvpp} \approx 0.0073 \left( \frac{m_p c^2}{13.6 \text{eV}} \right) f_H f_{burn} f_{uv} f_{esc}, \quad (2)$$

where

$$\begin{cases} f_H & = \text{mass fraction hydrogen in IGM,} \\ f_{burn} & = \text{mass fraction of hydrogen burnt,} \\ f_{uv} & = \text{fraction of energy released as UV photons,} \\ f_{esc} & = \text{fraction of UV photons that escape from galaxy.} \end{cases}$$

We will take the primordial mass fraction of helium to be 24%, *i.e.*  $f_H = 76\%$ . Now define the *net efficiency*

$$f_{net} = f_{burn} f_{uv} f_{esc} f_{ion},$$

and equation (1) becomes

$$\chi \approx 3.8 \times 10^5 f_{net} f_s. \quad (3)$$

The key feature to note about this expression is that since  $3.8 \times 10^5$  is such a large number, quite modest efficiencies  $f_{net}$  still allow  $\chi$  to become of order unity as soon as a very small fraction of the baryons are in galaxies. As will be seen in the next section, this means that reionization is possible even at redshifts far out in the Gaussian tail of the distribution of formation redshifts, at epochs long before those when the bulk of the baryons go nonlinear. This appears to have been first pointed out by Couchman and Rees (1986).

## 2 The Mass Fraction in Galaxies

In this section, we will discuss the parameter  $f_s$ . Assuming the standard PS theory of structure formation (Press & Schechter 1974), the fraction of all mass that has formed gravitationally bound objects of total (baryonic and non-baryonic) mass greater than  $M$  at redshift  $z$  is the integral of the Gaussian tail,

$$f_s = \text{erfc} \left[ \frac{\delta_c}{\sqrt{2}\sigma(M, z)} \right], \quad (4)$$

where the complementary error function  $\text{erfc}(x) \equiv 2\pi^{-1/2} \int_x^\infty e^{-u^2} du$  and  $\sigma(M, z)$  is the r.m.s. mass fluctuation in a sphere containing an expected mass  $M$  at redshift  $z$ .  $\sigma^2$  is given by top-hat filtering of the power spectrum as

$$\sigma(M, z)^2 \propto \int_0^\infty P(k) \left[ \frac{\sin kr_0}{(kr_0)^3} - \frac{\cos kr_0}{(kr_0)^2} \right]^2 dk, \quad (5)$$

where  $P(k)$  is the power spectrum at redshift  $z$  and  $r_0$  is given by  $\frac{4}{3}\pi r_0^3 \rho = M$ ,  $\rho = \frac{3H^2\Omega}{8\pi G}$  being the density of the universe at redshift  $z$ . Although this approach has been criticized as too simplistic, numerical simulations (Efstathiou *et al.* 1988; Efstathiou & Rees 1988; Carlberg & Couchman 1989) have shown that it describes the mass distribution of newly formed structures remarkably well. Making the standard assumption of a Gaussian density field, Blanchard *et al.* (1992) have argued that it is an accurate description at least in the low mass limit. Since we are mainly interested in extremely low masses such as  $10^6 M_\odot$ , it appears to suffice for our purposes.

For our middle-of-the road estimate, we choose  $\delta_c = 1.69$ , which is the linearly extrapolated overdensity at which a spherically symmetric perturbation has collapsed into a virialized object (Gott & Rees 1975; Efstathiou *et al.* 1988; Brainerd & Villumsen 1992). We take  $\delta_c = 1.44$  (Carlberg & Couchman 1989) for the optimistic estimate, although the even lower value  $\delta_c = 1.33$  has been discussed (Efstathiou & Rees 1988), and  $\delta_c = 2.00$  (Gelb & Bertschinger 1992) for the pessimistic estimate. (Here and throughout this paper, parameter choices are referred to as optimistic if they permit earlier reionization.)

The fact that  $\sigma(M, z) \rightarrow \infty$  as  $M \rightarrow 0$  implies that if we consider arbitrarily small scales, then all dark matter is in non-linear structures. Thus if no forces other than gravity were at work, so that the baryons always followed the dark matter, we would simply have  $f_s = 1$  at all  $z$ . However, it is commonly believed that galaxies correspond only to objects

that are able to cool (and fragment into stars) in a dynamical time or a Hubble time (Binney 1977; Rees & Ostriker 1977; Silk 1977; White & Rees 1978). The former applies to ellipticals and bulges, the latter to disks. Let us define the *virialization redshift*  $(1 + z_{vir}) \equiv (\sqrt{2}/\delta_c)\sigma(M_c, 0)$ , where  $M_c$  is some characteristic cutoff mass which is the total mass (baryonic and dark) of the first galaxies to form.  $z_{vir}$  is roughly the redshift at which the bulk of all baryons goes non-linear. Using equation (4) and the fact that  $\sigma(M, z) = \sigma(M, 0)/(1 + z)$  in the linear regime of CDM, we thus have

$$f_s = \operatorname{erfc} \left[ \frac{1 + z}{1 + z_{vir}} \right]. \quad (6)$$

A common assumption is that  $M_c \approx 10^6 M_\odot$ , roughly the Jeans mass at recombination. Blanchard *et al.* (1992) examine the interplay between cooling and gravitational collapse in considerable detail, and conclude that the first galaxies to form have masses in the range  $10^7 M_\odot$  to  $10^8 M_\odot$ , their redshift distribution still being given by equation (6), whereas Couchman & Rees (1986) argue that the first galaxies to form may have had masses as low as  $10^5 M_\odot$ .

As our CDM power spectrum today, we will use that given by BBKS (Bardeen *et al.* 1986) and an  $n = 1$  Harrison-Zel'dovich primordial spectrum:

$$P(k) \propto \left( \frac{q^{-1} \ln(1 + 2.34q)}{[1 + 3.89q + (16.1q)^2 + (5.46q)^3 + (6.71q)^4]^{1/4}} \right)^2 q,$$

where  $q \equiv k/[h^2 \Omega_0 \text{Mpc}^{-1}]$ . Throughout this paper, we will take  $\Omega_0 = 1$ .

Evaluating the  $\sigma^2$ -integral in equation (5) numerically yields

$$\sigma(10^5 M_\odot, 0) \approx 33.7b^{-1}$$

for  $h = 0.8$  and

$$\sigma(10^8 M_\odot, 0) \approx 13.6b^{-1}$$

for  $h = 0.5$ , where the so called bias factor  $b \equiv \sigma(8h^{-1} \text{Mpc}, 0)^{-1}$  has been estimated to lie between 0.8 (Smoot *et al.* 1992) and 2.5 (Bardeen *et al.* 1986). Our pessimistic, middle-of-the-road and optimistic CDM estimates of  $z_{vir}$  are given in Table 1, and the dependence of  $z_{vir}$  on  $M_c$  is plotted in Figure 1. This figure also shows three alternative models of structure formation: CDM with cosmological constant (Efstathiou *et al.* 1992); tilted CDM (Cen *et al.* 1992) and MDM, mixed hot and dark matter (Shafi & Stecker 1984; Schaefer & Shafi 1992; Davis *et al.* 1992; Klypin *et al.* 1993).

For the model with cosmological constant, we have taken a flat universe with  $h = 0.5$ ,  $\Omega_0 = 0.4$  and  $\lambda_0 = 0.6$ . For the tilted model, the power spectrum  $P(k)$  is simply multiplied by a factor  $k^{n-1}$ , where we have taken  $n = 0.7$ . For the tilted case, equation (6) still applies. For the MDM case, however, perturbations in the cold component grow slower than linearly with the scale factor  $(1+z)^{-1}$  and equation (6) is not valid. For the low masses we are considering, we have (Bond & Szalay 1983)

$$\sigma_{MDM}(M_c, z) \approx \frac{\sigma_{MDM}(M_c, 0)}{(1+z)^\alpha}, \quad \text{where}$$

$$\alpha \equiv \frac{1}{4} \left[ \sqrt{25 - 24\Omega_{HDM}} - 1 \right].$$

Using the parameters from Davis *et al.* (1992), who take  $\Omega = 1$  and  $\Omega_{HDM} = 0.3$ , the MDM version of equation (6) becomes

$$f_s = \text{erfc} \left[ \left( \frac{1+z}{1+z_{vir}} \right)^\alpha \right]$$

where  $\alpha \approx 0.8$  and we redefine  $z_{vir}$  by

$$(1+z_{vir}) \approx \left[ \frac{\sqrt{2}\sigma(M_c, 0)}{5.6\delta_c} \right]^{1/\alpha},$$

with  $\sigma(M_c, 0)$  referring to a pure CDM power spectrum.

For the  $\Lambda$  case, perturbations grow approximately linearly until the universe becomes vacuum dominated at  $z \approx \Omega_0^{-1} - 1 = 1.5$ , after which their growth slowly grinds to a halt. A numerical integration of the Friedmann equation and the equation for perturbation growth using  $h = 0.5$ ,  $\Omega_0 = 0.4$  and  $\lambda_0 = 0.6$  gives

$$\sigma_\Lambda(M_c, z) \approx 1.2 \frac{\sigma(M_c, 0)}{(1+z)}$$

for  $z \gg 3$ .

Since our  $\Lambda$ -model yields a value of  $z_{vir}$  very similar to our tilted model, we will omit the former from future plots.

### 3 Efficiency Parameters

In this section, we will discuss the various parameters that give  $f_{net}$  when multiplied together. The conclusions are summarized in Table 2.

|            | Mixed          | Tilted         | Lambda         | Pess.          | Mid.           | Opt.           |
|------------|----------------|----------------|----------------|----------------|----------------|----------------|
| $M_c$      | $10^6 M_\odot$ | $10^6 M_\odot$ | $10^6 M_\odot$ | $10^8 M_\odot$ | $10^6 M_\odot$ | $10^5 M_\odot$ |
| Model      | MDM            | Tilted         | Lambda         | CDM            | CDM            | CDM            |
| $h$        | 0.5            | 0.5            | 0.5            | 0.5            | 0.5            | 0.8            |
| $b$        | 1              | 1              | 1              | 2              | 1              | 0.8            |
| $\delta_c$ | 1.69           | 1.69           | 1.69           | 2.00           | 1.69           | 1.44           |
| $z_{vir}$  | 2.9            | 10.1           | 8.4            | 4.8            | 17.2           | 41.4           |

Table 1: Galaxy formation assumptions

|            | Pess.              | Mid.               | Opt.               |
|------------|--------------------|--------------------|--------------------|
| $f_{burn}$ | 0.2%               | 1%                 | 25%                |
| $f_{esc}$  | 10%                | 20%                | 50%                |
| $f_{uv}$   | 5%                 | 25%                | 50%                |
| $f_{ion}$  | 10%                | 40%                | 95%                |
| $f_{net}$  | $1 \times 10^{-6}$ | $2 \times 10^{-4}$ | $6 \times 10^{-2}$ |
| $f_{uvpp}$ | 4                  | 190                | 24,000             |

Table 2: Efficiency parameters used

| UV source       | Spectrum $P(\nu)$            | $f_{uv}$ | $\langle E_{uv} \rangle$ | $T^*$   | $\sigma_{18}$ |
|-----------------|------------------------------|----------|--------------------------|---------|---------------|
| O3 star         | $T = 50,000\text{K}$ Planck  | 0.57     | 17.3 eV                  | 28,300K | 2.9           |
| O6 star         | $T = 40,000\text{K}$ Planck  | 0.41     | 16.6 eV                  | 23,400K | 3.4           |
| O9 star         | $T = 30,000\text{K}$ Planck  | 0.21     | 15.9 eV                  | 18,000K | 3.9           |
| Pop. III star   | $T = 50,000\text{K}$ Vacca   | 0.56     | 18.4 eV                  | 36,900K | 2.2           |
| Black hole, QSO | $\alpha = 1$ power law       |          | 18.4 eV                  | 37,400K | 1.7           |
| ?               | $\alpha = 2$ power law       |          | 17.2 eV                  | 27,800K | 2.7           |
| ?               | $\alpha = 0$ power law       |          | 20.9 eV                  | 56,300K | 0.6           |
| ?               | $T = 100,000\text{K}$ Planck | 0.89     | 19.9 eV                  | 49,000K | 1.6           |

Table 3: Spectral parameters

$f_{burn}$ , the fraction of galactic hydrogen that is burnt into helium during the early life of the galaxy (within a small fraction of a Hubble after formation), is essentially the galactic metallicity after the first wave of star formation. Thus it is the product of the fraction of the hydrogen that forms stars and the average metallicity per star (weighted by mass). This depends on the stellar mass function, the galactic star formation rate and the final metallicities of the high-mass stars. For our middle-of-the-road estimate, we follow Miralda-Escudé & Ostriker (1990) in taking  $f_{burn} = 1\%$ , half the solar value. An upper limit to  $f_{burn}$  is obtained from the extreme scenario where all the baryons in the galaxy form very massive and short-lived stars with  $M \approx 30M_{\odot}$ , whose metallicity could get as high as 25% (Woosley & Weaver 1986). Although perhaps unrealistic, this is not ruled out by the apparent absence of stars with such metallicities today, since stars that massive would be expected to collapse into black holes.

In estimating  $f_{esc}$ , the fraction of the UV photons that despite gas and dust manage to escape from the galaxy where they are created, we follow Miralda-Escudé & Ostriker (1990).

For  $f_{uv}$ , the fraction of the released energy that is radiated above the Lyman limit, we also follow Miralda-Escudé & Ostriker (1990). The upper limit refers to the extreme  $30M_{\odot}$  scenario mentioned above. For reference, the values of  $f_{uv}$  for stars with various spectra are given in Table 3, together with some other spectral parameters that will be defined and used in the appendix. All these parameters involve spectral integrals, and have been computed numerically.

The parameter  $f_{ion}$  is estimated in the appendix.

An altogether different mechanism for converting the baryons in non-linear structures into ultraviolet photons is black hole accretion. If this mechanism is the dominant one, equation (2) should be replaced by

$$f_{uvpp} \approx \left( \frac{m_p c^2}{13.6 \text{eV}} \right) f_{bh} f_{acc} f_{uv} f_{esc},$$

where

$$\begin{cases} f_{bh} & = \text{mass fraction of nonlinear structures that end up as black holes,} \\ f_{acc} & = \text{fraction of rest energy radiated away during accretion process,} \\ f_{uv} & = \text{fraction of energy released as UV photons,} \\ f_{esc} & = \text{fraction of UV photons that escape from host galaxy.} \end{cases}$$

There is obviously a huge uncertainty in the factor  $f_{bh}$ . However, the absence of the factor  $0.0073 \times 0.76$  compared to equation (2) means that the conversion of matter into radiation is so much more efficient that the black hole contribution might be important even if  $f_{bh}$  is quite small. For instance,  $f_{acc} = 10\%$  and  $f_{esc} = 100\%$  gives  $f_{uvpp} \approx 10^8 f_{bh} f_{uv}$ , which could easily exceed the optimistic value  $f_{uvpp} \approx 24,000$  for the stellar burning mechanism in Table 2.

In Figure 2, the ionization fraction  $\chi(z)$  is plotted for various parameter values using equations (1) and (6). It is seen that the ionization grows quite abruptly, so that we may speak of a fairly well-defined *ionization redshift*. Let us define the ionization redshift  $z_{ion}$  as the redshift when  $\chi$  becomes 0.5, *i.e.*

$$1 + z_{ion} = (1 + z_{vir}) \text{erfc}^{-1} \left( \frac{1}{2f_{uvpp} f_{ion}} \right). \quad (7)$$

This dependence of  $z_{ion}$  of the efficiency is shown in Figure 3 for our various galaxy formation scenarios. It is seen that the ionization redshift is fairly insensitive to the net efficiency, with the dependence being roughly logarithmic for  $f_{net} > 0.0001$ .

## 4 Scattering History

For a given ionization history  $\chi(z)$ , the Thomson opacity out to a redshift  $z$ , the probability that a CBR photon is Thomson scattered at least once after  $z$ , is

$$P_s(z) = 1 - e^{-\tau(z)},$$

where the optical depth for Thomson scattering is given by

$$\begin{cases} \tau(z) &= \tau^* \int_0^z \frac{1+z'}{\sqrt{1+\Omega_0 z'}} \chi(z') dz', \\ \tau^* &= \frac{3\Omega_b}{8\pi} \left[ 1 - \left( 1 - \frac{x_{He}}{4x} \right) f_{He} \right] \frac{H_0 c \sigma_t}{m_p G} \approx 0.057 h \Omega_b, \end{cases}$$

where we have taken the mass fraction of helium to be  $f_{He} \approx 24\%$  and assumed  $x_{He} \approx x$ , *i.e.* that helium never becomes doubly ionized and that the fraction that is singly ionized equals the fraction of hydrogen that is ionized. The latter is a very crude approximation, but makes a difference of only 6%. We assume that  $\Omega_0 = 1$  throughout this paper.  $\Omega_b$  denotes the density of the intergalactic medium divided by the critical density, and is usually assumed to equal  $\Omega_b$ , the corresponding density of baryons. the probability that a CBR photon is Thomson scattered at least once after the standard recombination epoch at  $z \approx 10^3$ .

The profile of the last scattering surface is given by the so called visibility function

$$f_z(z) \equiv \frac{dP_s}{dz}(z),$$

which is the probability distribution for the redshift at which a photon last scattered. An illuminating special case is that of complete ionization at all times, *i.e.*  $\chi(z) = 1$ , which yields

$$P_s(z) = 1 - \exp\left(-\frac{2}{3}\tau^* \left[(1+z)^{3/2} - 1\right]\right) \approx 1 - \exp\left[-\left(\frac{z}{92}\right)^{3/2}\right] \quad (8)$$

for  $z \gg 1$  and  $h\Omega_b = 0.03$ . Hence we see that in order for any significant fraction of the CBR to have been rescattered by reionization, the reionization must have occurred quite early. Figures 4 and 5 show the opacity and last-scattering profile for three different choices of  $h\Omega_b$ . In the optimistic case  $h\Omega_b = 0.1$ , it is seen that even as low an ionization redshift as  $z_{ion} = 30$  would give a total opacity  $P_s \approx 50\%$ . In Figures 6 and 7, we have replaced  $z$  by the angle subtended by the horizon radius at that redshift,

$$\theta(z) = 2 \arctan \left[ \frac{1}{2(\sqrt{1+z} - 1)} \right],$$

which is the largest angular scale on which Thomson scattering at  $z$  would affect the microwave background radiation. In Figure 7, we have plotted the

angular visibility function  $dP_s/d(-\theta)$  instead of  $dP_s/dz$ , so that the curves are probability distributions over angle instead of redshift.

In the *sudden approximation*, the ionization history is a step function

$$\chi(z) = \theta(z_{ion} - z)$$

for some constant  $z_{ion}$ , and as was discussed in Section 3, this models the actual ionization history fairly well. In this approximation, the visibility functions are identical to those in Figures 5 and 7 for  $z < z_{ion}$ , but vanish between  $z_{ion}$  and the recombination epoch at  $z \approx 10^3$ . Figure 8, which is in a sense the most important plot in this paper, shows the total opacity  $P_s(z_{ion})$  as a function of  $f_{net}$  for a variety of parameter values, as obtained by substituting equation (7) into (8). As can be seen, the resulting opacity is relatively insensitive to the poorly known parameter  $f_{net}$ , and depends mainly on the structure formation model (*i.e.*  $z_{vir}$ ) and the cosmological parameter  $h\Omega_b$ .

Thomson scattering between CBR photons and free electrons affects not only the spatial but also the spectral properties of the CBR. It has long been known that hot ionized IGM causes spectral distortions to the CBR, known as the Sunyaev-Zel'dovich effect. A useful measure of this distortion is the Comptonization  $y$ -parameter (Kompanéets 1957; Zel'dovich & Sunyaev 1969; Stebbins & Silk 1986; Bartlett & Stebbins 1991)

$$y_c = \int \left( \frac{kT}{m_e c^2} \right) n_e \sigma_t c dt,$$

where the integral is to be taken from the reionization epoch to today. Let us estimate this integral by making the approximation that the IGM is cold and neutral until a redshift  $z_{ion}$ , at which it suddenly becomes ionized, and after which it remains completely ionized with a constant temperature  $T$ . Then for  $\Omega = 1$ ,  $z_{ion} \gg 1$ , we obtain

$$y_c = \left( \frac{kT}{m_e c^2} \right) \left( \frac{n_{e0} \sigma_t c}{H_0} \right) \int_0^{z_{ion}} \sqrt{1+z} dz \approx 6.4 \times 10^{-8} h\Omega_b T_4 z_{ion}^{3/2},$$

where  $T_4 \equiv T/10^4\text{K}$  and  $n_{e0}$ , the electron density today, has been computed as before assuming a helium mass fraction of 24% that is singly ionized. Substituting the most recent observational constraint from the COBE FIRAS experiment,  $y_c < 2.5 \times 10^{-5}$  (Mather *et al.* 1994), into this expression yields

$$z_{ion} < 554 T_4^{-2/3} \left( \frac{h\Omega_b}{0.03} \right)^{-2/3},$$

so all our scenarios are consistent with this spectral constraint.

## 5 Discussion

A detailed discussion of how reionization affects the microwave background anisotropies would be beyond the scope of this paper, so we will merely review the main features. If the microwave background photons are rescattered at a redshift  $z$ , then the fluctuations we observe today will be suppressed on angular scales smaller than the angle subtended by the horizon at that redshift. This effect is seen in numerical integrations of the linearized Boltzmann equation (*e.g.* Bond & Efstathiou 1984; Vittorio & Silk 1984), and can be simply understood in purely geometrical terms. Suppose we detect a microwave photon arriving from some direction in space. Where was it just after recombination? In the absence of reionization, it would have been precisely where it appears to be coming from, say 3000 Mpc away. If the IGM was reionized, however, the photon might have originated somewhere else, scattered off of a free electron and then started propagating towards us, so at recombination it might even have been right here. Thus to obtain the observed anisotropy, we have to convolve the anisotropies at last scattering with a window function that incorporates this smoothing effect. Typical widths for the window function appropriate to the last scattering surface range from a few arc-minutes with standard recombination to the value of a few degrees that we have derived here for early reionization models.

In addition to this suppression on sub-horizon scales, new fluctuations will be generated by the first order Doppler effect and by the Vishniac effect. The latter dominates on small angular scales and is not included in the linearized Boltzmann treatment because it is a second order effect. The current upper limit on CBR fluctuations on the 1 arcminute scale of  $\Delta T/T < 9 \times 10^{-6}$  (Subrahmanyan *et al.* 1993) provides an interesting constraint on reionization histories through the Vishniac effect. In fact, according to the original calculations (Vishniac 1987), this would rule out most of the reionization histories in this paper. However, a more careful treatment (Hu *et al.* 1994) predicts a Vishniac effect a factor of five smaller on this angular scale, so all reionization histories in this paper are still permitted.

The COBE DMR detection of  $\Delta T/T$  has provided a normalization for predicting CBR anisotropies on degree scales. Several experiments are underway to measure such anisotropies, and early results that report possible detections have recently become available from experiments at the South Pole (Meinhold & Lubin 1991; Shuster *et al.* 1993) and at balloon altitudes (Devlin *et al.* 1992; Meinhold *et al.* 1993; Shuster *et al.* 1993). There is some reason to believe that these detected signals are contaminated by galactic

emission. Were this the case, the inferred CBR upper limits to fluctuations on degree scales might be lower than those predicted from COBE extrapolations that adopt the scale-invariant power spectrum that is consistent with the DMR result and is generally believed to be the most appropriate choice on large scales from theoretical considerations (*e.g.* Gorski *et al.* 1993; Kashlinsky 1992). In the absence of such contaminations, the detected fluctuations in at least some degree-scale experiments are, however, consistent with the COBE extrapolation (*e.g.* Jubas & Dodelson 1993). The variation from field to field, repeated on degree scales, also may argue either for galactic contamination or else for unknown experimental systematics, or even non-Gaussian fluctuations. The results of other recent experiments such as ARGO (de Bernardis *et al.* 1993), PYTHON (Dragovan *et al.* 1993) and MSAM (Cheng *et al.* 1993) have reinforced the impression that the experimental data is not entirely self-consistent, and that some form of systematic errors may be important.

The controversy over the interpretation of the degree-scale CBR fluctuations makes our reanalysis of the last scattering surface particularly timely. We have found that canonical dark matter, tailored to provide the 10 degree CBR fluctuations detected by the COBE DMR experiment, results in sufficiently early reionization (before  $z \approx 50$ ) over a fairly wide range of parameter space, to smooth out primordial degree-scale fluctuations. Our middle-of-the-road model produces suppression by roughly a factor of two; it is difficult, although not impossible, to obtain a much larger suppression. This smoothing, because it is of order unity in scattering optical depth, is necessarily inhomogeneous. We predict the presence of regions with large fluctuations and many “hot spots” and “cold spots”, corresponding to “holes” in the last-scattering surface, as well as regions with little small-scale power where the last scattering is more efficient. The detailed structure of the CBR sky in models with reionization will be left for future studies. Here we simply conclude by emphasizing that anomalously low values of  $\Delta T/T$  over degree scales are a natural corollary of reionization at high redshift.

## A Appendix: The Efficiency Parameter $f_{ion}$

In this appendix, we will discuss the parameter  $f_{ion}$ , and see that it rarely drops below 30%. We will first discuss the thermal evolution of intergalactic hydrogen exposed to a strong UV flux, and then use the results to write down

a differential equation for the volume fraction of the universe that is ionized, subject to point sources of UV radiation that switch on at different times. We will see that photoionization is so efficient within the ionized regions of the IGM that quite a simple equation can be given for the expansion of the ionized regions.

The evolution of IGM exposed to ionizing radiation has been discussed by many authors. Important early work includes that of Arons & McCray (1970), Bergeron & Salpeter (1970) and Arons & Wingert (1972). The main novelty of the treatment that follows is that whereas previous treatments focus on late ( $z < 5$ ) epochs, when various simplifying approximations can be made because the recombination and Compton rates are low, we are mainly interested in the case  $50 < z < 150$ . We show that IGM exposed to a strong UV flux rapidly approaches a quasistatic equilibrium state, where it is almost fully ionized and the temperature is such that photoionization heating exactly balances Compton cooling. This simplifies the calculations dramatically, since the entire thermal history of the IGM can be summarized by a single function  $\chi(z)$ , the volume fraction that is ionized. Thus a fraction  $\chi(z)$  is ionized and hot (with a temperature that depends only on  $z$ , not on when it became ionized), and a fraction  $1 - \chi(z)$  is neutral and cold.

In the first section, we justify this approximation. In the second section, we derive a differential equation for the time-evolution of  $\chi$  as well as a useful analytic estimate of  $f_{ion}$ .

## A.1 Intergalactic Strömgren Spheres

Let  $x$  denote the ionization fraction in a small, homogeneous volume of intergalactic hydrogen, *i.e.*  $x \equiv n_{HII}/(n_{HI} + n_{HII})$ . ( $x$  is not to be confused with  $\chi$ , the volume fraction in ionized bubbles.) When this IGM is at temperature  $T$ , exposed to a density of  $\eta$  UV photons per proton, the ionization fraction  $x$  evolves as follows:

$$\frac{dx}{d(-z)} = \frac{1+z}{\sqrt{1+\Omega_0 z}} \left[ \lambda_{pi}(1-x) + \lambda_{ci}x(1-x) - \lambda_{rec}^{(1)}x^2 \right], \quad (9)$$

where  $H_0^{-1}(1+z)^{-3}$  times the rates per baryon for photoionization, collisional ionization and recombination are given by

$$\begin{cases} \lambda_{pi} \approx 1.04 \times 10^{12} [h\Omega_b\sigma_{18}] \eta, \\ \lambda_{ci} \approx 2.03 \times 10^4 h\Omega_b T_4^{1/2} e^{-15.8/T_4}, \\ \lambda_{rec}^{(1)} \approx 0.717 h\Omega_b T_4^{-1/2} [1.808 - 0.5 \ln T_4 + 0.187 T_4^{1/3}], \end{cases} \quad (10)$$

and  $T_4 \equiv T/10^4\text{K}$ .  $\sigma_{18}$  is the thermally averaged photoionization cross section in units of  $10^{-18}\text{cm}^2$ , and has been computed in Table 3 for various spectra using the differential cross section from Osterbrock (1974). The collisional ionization rate is from Black (1981). The recombination rate is the total rate to all hydrogenic levels (Seaton 1959).

Below we will see that in the ionized Strömngren bubbles that will appear around the galaxies or quasars, the photoionization rate is so much greater than the other rates that to a good approximation, equation (9) can be replaced by the following simple model for the IGM:

- It is completely ionized ( $x = 1$ ).
- When a neutral hydrogen atom is formed through recombination, it is instantly photoionized again.

Thus the only unknown parameter is the IGM temperature, which determines the recombination rate, which in turn equals the photoionization rate and thus determines the rate of heating.

Let us investigate when this model is valid. Near the perimeter of an ionized Strömngren sphere of radius  $r$  surrounding a galaxy, the number of UV photons per proton is roughly

$$\eta = \frac{S_{uv}}{4\pi r^2 cn},$$

where  $S_{uv}$  is the rate at which UV photons leave the galaxy. For an O5 star, the photon flux above the Lyman limit is approximately  $3.1 \times 10^{49}\text{s}^{-1}$  (Spitzer 1968), so if each  $N$  solar masses of baryons in a galaxy leads to production of a UV flux equivalent to that of an O5 star, then

$$\eta \geq 0.77 \frac{f_{esc} M_6}{h^2 r_1^2 N (1+z)^3}, \quad (11)$$

inside the sphere, where  $r_1 \equiv r/1\text{Mpc}$  and  $M_6 \equiv M/10^6 M_\odot$ . When a fraction  $f_s$  of all matter has formed galaxies of a typical total (baryonic and dark) mass  $M$ , then in the absence of strong clustering, the typical separation between two galaxies is

$$R = \left( \frac{M}{f_s \rho} \right)^{1/3} \approx \left( \frac{15\text{kpc}}{1+z} \right) \left( \frac{M_6}{h^2 f_s} \right)^{1/3},$$

where  $M_6 \equiv M/10^6 M_\odot$ . Thus  $r$  continues to increase until  $r \approx R$ , and spheres from neighboring galaxies begin to overlap. We are interested in the regime where  $z < 150$ . Substituting this and equation (11) into (10),

we see that  $\lambda_{pi} \gg \lambda_{ci}$  and  $\lambda_{pi} \gg \lambda_{rec}$  for any reasonable parameter values. Hence we can neglect collisional ionization in equation (9). Since  $\lambda_{pi} \gg 1$ , the photoionization timescale is much shorter than the Hubble timescale, so equation (9) will quickly approach a quasistatic equilibrium solution where the recombination rate equals the photoionization rate, *i.e.*

$$x \approx 1 - \frac{\lambda_{rec}}{\lambda_{pi}} \approx 1.$$

In conclusion, the simple  $x = 1$  model is valid for all parameter values in our regime of interest.

When a hydrogen atom gets ionized, the photoelectron acquires an average kinetic energy of  $\frac{3}{2}kT^*$ , where  $T^*$  is defined by  $\frac{3}{2}kT^* = \langle E_{uv} \rangle - 13.6\text{eV}$ , and  $\langle E_{uv} \rangle$  is the average energy of the ionizing photons (see Table 3).

Since the timescale for Coulomb collisions is much shorter than any other timescales involved, the electrons and protons rapidly thermalize, and we can always assume that their velocity distribution is Maxwellian, corresponding to some well-defined temperature  $T$ . Thus shortly after the hydrogen gets photoionized, after the electrons have transferred half of their energy to the protons, the plasma temperature is  $T = \frac{1}{2}T^*$ .

The net effect of a recombination and subsequent photoionization is to remove the kinetic energy of the captured electron, say  $\frac{3}{2}kT\eta_{rec}(T)$ , from the gas and replace it with  $\frac{3}{2}kT^*$ , the kinetic energy of the new photoelectron. Since the recombination cross section is approximately proportional to  $v^{-2}$ , slower electrons are more likely to get captured. Hence the mean energy of the captured electrons is slightly lower than  $\frac{3}{2}kT$ , *i.e.*  $\eta_{rec}(T)$  is slightly less than unity (Osterbrock 1974). We compute  $\eta_{rec}(T)$  using Seaton (1959). The complication that  $\eta_{rec}(T) \neq 1$  turns out to be of only marginal importance:  $\eta_{rec}(10^4\text{K}) \approx 0.8$ , which only raises the equilibrium temperatures calculated below by a few percent.

The higher the recombination rate, the faster this effect will tend to push the temperature up towards  $T^*$ . The two dominant cooling effects are Compton drag against the microwave background photons and cooling due to the adiabatic expansion of the universe. Line cooling from collisional excitations can be neglected, since the neutral fraction  $1 - x \approx 0$ . Combining these effects, we obtain the evolution equation for the IGM inside of a Strömngren bubble:

$$\frac{dT}{d(-z)} = -\frac{2}{1+z}T + \frac{1+z}{\sqrt{1+\Omega_0 z}} \left[ \lambda_{comp}(T_{cbr} - T) + \frac{1}{2}\lambda_{rec}(T)[T_{cbr} - \eta_{rec}(T)T] \right] \quad (12)$$

where

$$\lambda_{comp} = \frac{4\pi^2}{45} \left( \frac{kT_{cbr}}{\hbar c} \right)^4 \frac{\hbar\sigma_t}{H_0 m_e} (1+z)^{-3} \approx 0.00418 h^{-1} (1+z)$$

is  $(1+z)^{-3}$  times the Compton cooling rate per Hubble time and  $T_{cbr} = T_{cbr,0}(1+z)$ . We have taken  $T_{cbr,0} \approx 2.726\text{K}$  (Mather *et al.* 1994). The factor of  $\frac{1}{2}$  in front of the  $\lambda_{rec}$  term is due to the fact that the photoelectrons share their acquired energy with the protons. The average energy of the ionizing photons is given by the spectrum  $P(\nu)$  as  $\langle E_{uv} \rangle = h\langle \nu \rangle$ , where

$$\langle \nu \rangle = \frac{\int_0^\infty P(\nu)\sigma(\nu)d\nu}{\int_0^\infty \nu^{-1}P(\nu)\sigma(\nu)d\nu}.$$

Here the photoionization cross section  $\sigma(\nu)$  is given by Osterbrock (1974). Note that, in contrast to certain nebula calculations where all photons get absorbed sooner or later, the spectrum should be weighted by the photoionization cross section. This is because most photons never get absorbed in the Strömgen regions (only in the transition layer), and all that is relevant is the energy distribution of those photons that do.  $P(\nu)$  is the energy distribution (W/Hz), not the number distribution which is proportional to  $P(\nu)/\nu$ .

The spectral parameters  $\langle E_{uv} \rangle$  and  $T^*$  are given in Table 3 for some selected spectra. A Planck spectrum  $P(\nu) \propto \nu^3 / (e^{h\nu/kT} - 1)$  gives quite a good prediction of  $T^*$  for stars with surface temperatures below 30,000K. For very hot stars, more realistic spectra (Vacca, 1993) have a sharp break at the Lyman limit, and fall off much slower above it, thus giving higher values of  $T^*$ . As seen in Table 3, an extremely metal poor star of surface temperature 50,000K gives roughly the same  $T^*$  as QSO radiation. The only stars that are likely to be relevant to early photoionization scenarios are hot and short-lived ones, since the universe is only about  $10^7$  years old at  $z = 100$ , and fainter stars would be unable to inject enough energy in so short a time. Conceivably, less massive stars could play a dominant role later on, thus lowering  $T^*$ . However, since they radiate such a small fraction of their energy above the Lyman limit, very large numbers would be needed, which could be difficult to reconcile with the absence of observations of Population III stars today. If black holes are the dominant UV source, the stellar spectra of Table 3 are obviously irrelevant. A power law spectrum  $P(\nu) \propto \nu^{-\alpha}$  with  $\alpha = 1$  fits observed QSO spectra rather well in the vicinity of the Lyman limit (Cheney & Rowan-Robinson 1981; O'Brien *et al.* 1988), and is also consistent with the standard model for black hole accretion.

Numerical solutions to equation (12) are shown in Figure 9, and it is seen that the temperature evolution separates into three distinct phases. In the first phase, the IGM is outside of the Strömgen regions, unexposed to UV radiation, and remains cold and neutral. In the second phase, the IGM suddenly becomes ionized, and its temperature instantly rises to  $\frac{1}{2}T^*$ . After this, Compton cooling rapidly reduces the temperature to a quasi-equilibrium value of a few thousand K. After this, in the third phase,  $T$  changes only quite slowly, and is approximately given by setting the expression in square brackets in equation (12) equal to zero. This quasi-equilibrium temperature is typically many times lower than  $T^*$ , since Compton cooling is so efficient at the high redshifts involved.

## A.2 The Expansion of Strömgen Regions

This rapid approach to quasi-equilibrium, where the IGM “loses its memory” of how long ago it became part of a Strömgen region, enables us to construct a very simple model for the ionization history of the universe. At redshift  $z$ , a volume fraction  $\chi(z)$  of the universe is completely ionized and typically has a temperature of a few thousand K. The ionized part need not consist of non-overlapping spheres; it can have any topology whatsoever. The remainder is cold and neutral.

Between the ionized and neutral regions is a relatively thin transition layer, where the IGM becomes photoionized and its temperature adjusts to the quasistatic value as in Figure 9. As this IGM becomes part of the hot and ionized volume, the transition layer moves, and  $\chi(z)$  increases<sup>2</sup>.

As long as  $\chi < 1$ , all UV photons produced are absorbed instantly to a good approximation. Thus the rate at which UV photons are released is the sum of the rate at which they are used to counterbalance recombinations inside the hot bubbles and the rate at which they are used to break new ground, to increase  $\chi$ . Thus

$$f_{uvpp} \frac{df_s}{dt} = \alpha^{(2)}(T)n\chi + \frac{d\chi}{dt},$$

---

<sup>2</sup>We are tacitly assuming that the UV luminosity of the galaxy that creates each Strömgen sphere never decreases. Although obviously untrue, this is in fact an excellent approximation, since these early dwarf-galaxies correspond to perturbations far out in the Gaussian tail. Since  $f_s(z)$  grows so dramatically as the redshift decreases and we move from five sigma to four sigma to three sigma, *etc.*, almost all galaxies in existence at a given redshift are in fact very young, so that older ones that have begun to dim can be safely neglected.

where  $\alpha^{(2)}(T)$  is the total recombination rate to all hydrogenic levels except the ground state<sup>3</sup>. Changing the independent variable to redshift and using equation (6), we find that this becomes

$$\frac{d\chi}{d(-z)} + \lambda_{rec}^{(2)} \frac{1+z}{\sqrt{1+\Omega_0 z}} \chi = \frac{2}{\sqrt{\pi}} \left( \frac{f_{uvpp}}{1+z_{vir}} \right) \exp \left[ - \left( \frac{1+z}{1+z_{vir}} \right)^2 \right]. \quad (13)$$

Here

$$\lambda_{rec}^{(2)} \approx 0.717h\Omega_b T_4^{-1/2} \left[ 1.04 - 0.5 \ln T_4 + 0.19 T_4^{1/2} \right]$$

is  $H_0^{-1}(1+z)^{-3}$  times the total recombination rate per baryon to all hydrogenic levels except the ground state. The fit is to the data of Spitzer (1968) and is accurate to within 2% for  $30\text{K} < T < 64,000\text{K}$ .  $\lambda_{rec}^{(2)}$  is to be evaluated at the quasi-equilibrium temperature  $T(z)$  discussed above.

Using the values in Table 3 for the pessimistic, middle-of-the-road and optimistic estimates, the parameter  $f_{uvpp}$  equals roughly 4, 190 and 24,000, respectively.

In the absence of photon waste through recombination, equation equation (13) would have the solution  $\chi^*(z) = f_{uvpp} f_s(z)$ , so the ionization efficiency is

$$f_{ion}(z) = \chi(z)/\chi^*(z).$$

Since equation (13) is linear in  $\chi$  and the initial data is  $\chi = 0$  at some redshift, it is readily seen that the solution  $\chi(z)$  is proportional to  $f_{uvpp}$ , the constant in front of the source term. Combining these last two observations, we see that  $f_{ion}$  is independent of  $f_{uvpp}$  and hence independent of the poorly known parameters  $f_{burn}$ ,  $f_{uv}$  and  $f_{esc}$ .

Plots of  $f_{ion}(z)$  from numerical solutions of equation (13) are shown in Figure 10 for various parameter values, and it is seen that the dependence on  $z$  is generally quite weak. Let us make use of this fact by substituting the *Ansatz*  $\chi(z) = f_{ion}(z) f_{uvpp} f_s(z)$  into equation (13), and setting  $f'_{ion}(z) \approx 0$ . Using equation (6) and an asymptotic approximation for the error function,

---

<sup>3</sup>A reionization directly to the ground state produces a UV photon that usually propagates uninterrupted through the highly ionized Strömngren region, and then ionizes another atom in the transition layer between the expanding Strömngren region and its cold and neutral surrounding. Thus recombinations directly to the ground state were included in the above calculation of the quasi-equilibrium temperature of the Strömngren bubbles, since the resulting UV photons could be considered lost from the latter. Here, on the contrary, recombinations directly to the ground state should not be included, since the UV photons they produce are not wasted from an energetics point of view.

we obtain

$$f_{ion}(z) \approx \frac{1}{1 + 0.48\lambda_{rec}^{(2)}(1 + z_{vir})^2/\sqrt{1 + \Omega_0 z}},$$

independent of  $f_{uvpp}$ , which agrees to within 10% with the numerical solutions for all reasonable parameter values. This expression highlights the connection between  $f_{ion}$  and the thermal evolution of the Strömgren bubbles: Essentially, the higher the quasi-static temperature, the lower the recombination rate  $\lambda_{rec}^{(2)}$ , and the higher  $f_{ion}$  becomes.

The value of  $f_{ion}$  relevant to computing the ionization redshift is obviously that where  $z = z_{ion}$ . As we have seen,  $z_{ion}$  typically lies between  $2z_{vir}$  and  $3z_{vir}$ . Substituting  $T \approx 2,500\text{K}$  into the expression for  $\lambda_{rec}$  and taking  $\Omega_0 \approx 1$  and  $z = z_{ion} \approx 2.5z_{vir}$ , the above reduces to

$$f_{ion} \approx \frac{1}{1 + 0.8h\Omega_b(1 + z_{vir})^{3/2}},$$

so we see that  $f_{ion}$  will be of order unity unless  $z_{vir} \gg 15$  or  $h\Omega_b \gg 0.03$ .

The authors would like to thank Prof. A. Blanchard for illuminating discussions on the subject of the paper and W. Hu, A. Reisenegger, D. Schlegel, D. Scott and our referee for many useful comments. This research has been supported in part by a grant from the NSF.

## B REFERENCES

- Arons. J. & McCray, R. 1970, *Ap. Letters*, **5**, 123.  
Arons, J. & Wingert, D. 1972, *Ap. J.*, **177**, 1.  
Bardeen, J. M., Bond, J. R., Kaiser, N. & Szalay, A. S. 1986, *Ap. J.*, **304**, 15.  
Bartlett, J. & Stebbins, A. 1991, *Ap. J.*, **371**, 8.  
Bergeron, J. & Salpeter, E. 1970, *Ap. Letters*, **7**, 115.  
Binney, J. 1977, *Ap. J.*, **215**, 483.  
Black, J. 1981, *MNRAS*, **197**, 553.  
Blanchard, A., Valls-Gabaud, D. & Mamon, G. A. 1992, *Astr. Ap.*, **264**, 365.  
Bond, J. R. & Efstathiou, G. 1984, *Ap. J. (Letters)*, **285**, L45.  
Bond, J. R. & Szalay, A. S. 1983, *Ap. J.*, **274**, 443.  
Brainerd, T. G. & Villumsen, J. V. 1992, *Ap. J.*, **394**, 409.  
Carlberg, R. G. & Couchman, H. M. P. 1989, *Ap. J.*, **340**, 47.  
Cen, R., Gnedin, N. Y., Koffmann, L. A. & Ostriker, J. P. 1992, Preprint.  
Cheney, J. E. & Rowan-Robinson, M. 1981, *MNRAS*, **195**, 831.

- Couchman, H. M. P. & Rees, M. J. 1986, *MNRAS*, **221**, 53.
- Davis, M., Summers, F. J. & Schlegel, D. 1992, *Nature*, **359**, 393.
- Devlin, M. *et al.* 1992, in Proc. NAS Colloquium on Physical Cosmology, Physics Reports (in press).
- Efstathiou, G., Bond, J. R. & White, S. D. M. 1992, *MNRAS*, **258**, 1P.
- Efstathiou, G. & Rees, M. J. 1988, *MNRAS*, **230**, 5P.
- Efstathiou, G., Frenk, C. S., White, S. D. M., Davis, M. 1988, *MNRAS*, **235**, 715.
- Feynman, R. P. 1939, *Phys. Rev.*, **56**, 340.
- Gelb, J. M. & Bertschinger, E. 1992, preprint.
- Gorski, K., Juskiewicz, R. & Stompor, R. 1993, preprint.
- Gott, J. R. & Rees, M. J. 1975, *Astr. & Ap.*, **45**, 365.
- Gundersen, J. O. *et al.* 1993, preprint.
- Jubas, J. & Dodelson, S. 1993, preprint.
- Kashlinsky 1992, *Ap.J.*, **399**, L1..
- Klypin, A., Holtzman, J., Primack, J. & Regös, E. 1993, preprint.
- Kompanéets, A. 1957, *Soviet Phys. – JETP*, **4**, 730.
- Meinhold, P. R. & Lubin, P. M. 1991, *Ap. J.*, **370**, L11.
- Mather *et al.* 1993, preprint.
- Meinhold, P. R. *et al.* 1993, *Ap. J. Lett.*, submitted.
- Miralda-Escudé, J. & Ostriker, J. P. 1990, *Ap. J.*, **350**, 1.
- O’Brien P.T., Wilson, R & Gondhalekar, P. M 1988, *MNRAS*, **233**, 801.
- Osterbrock, D. E. 1974, *Astrophysics of Gaseous Nebulae* (Freeman, San Francisco).
- Press, W. H., & Schechter, P. 1974, *Ap. J.*, **187**, 425.
- Rees, M. J., & Ostriker, J. P. 1977, *MNRAS*, **179**, 541.
- Rees, M. J. 1986, *MNRAS*, **218**, 25P.
- Seaton, M. 1959, *MNRAS*, **119**, 84.
- Shaefer, R. K. & Shafi, Q. 1992, *Nature*, **359**, 199.
- Shafi, Q. & Stecker, F. W. 1984, *Phys. Rev. Lett.*, **53**, 1292.
- Shuster, J. *et al.* 1993, private communication.
- Silk, J. I. 1977, *Ap. J.*, **211**, 638.
- Smoot, G. F. *et al.* 1992, *Ap. J. (Letters)*, **396**, L1-L18.
- Spitzer, L. 1968, *Diffuse Matter in Space* (Wiley, New York).
- Stebbins, A., & Silk, J. 1986, *Ap. J.*, **300**, 1.
- Subramanyan, R. *et al.* 1993, *MNRAS* (in press).
- Tegmark, M., Silk, J. & Evrard, A. 1993, *Ap. J.* (in press).
- W. Vacca 1993, private communication.
- Vishniac, E. 1987, *Ap. J.*, **322**, 597.
- Vittorio, N. & Silk, J. 1984, *Ap. J. (Letters)*, **285**, L39.

White, S. D. M., & Rees, M. J. 1986, *MNRAS*, **183**, 341.  
Zel'dovich, Y., & Sunyaev, R. 1969, *Ap. Space Sci.*, **4**, 301.

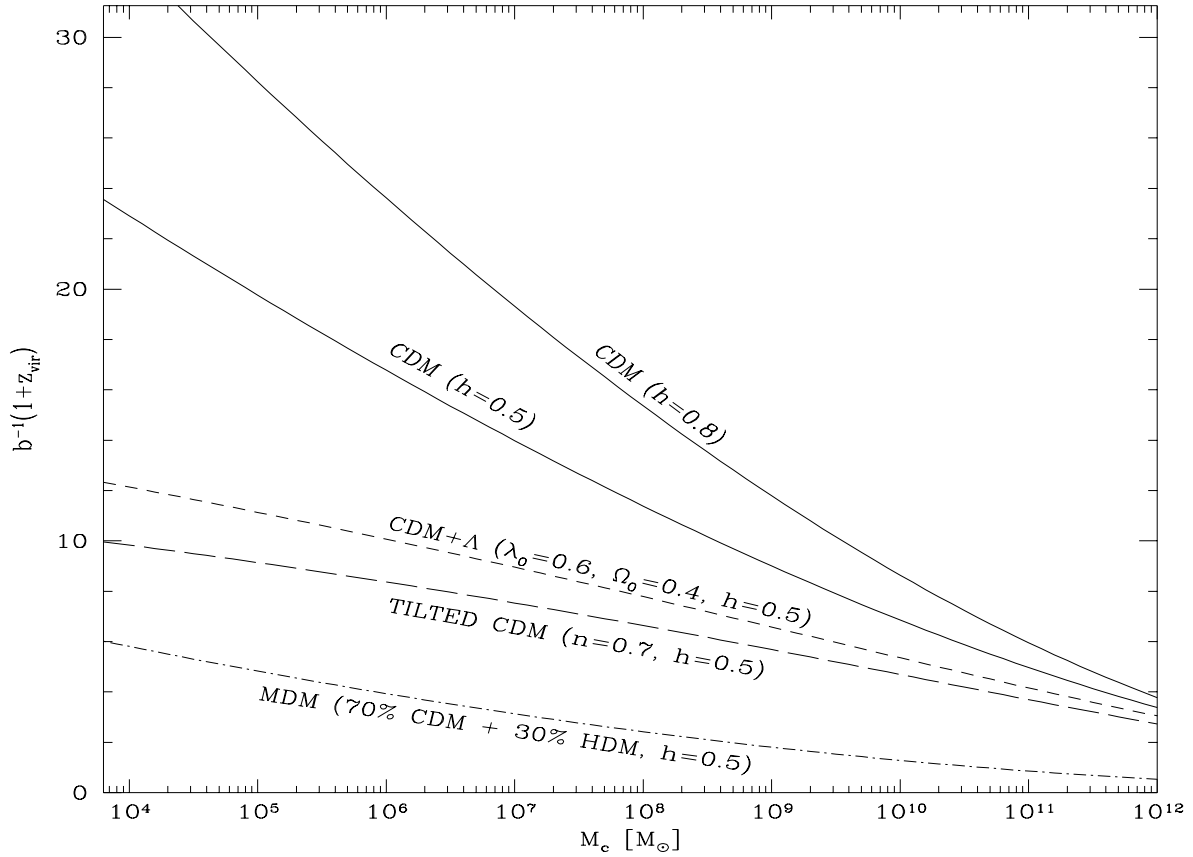


Figure 1: Virialization redshifts for objects of various masses. The virialization redshift, the redshift at which the bulk of the objects of mass  $M_c$  form, is plotted for a number of cosmological models. In all cases shown,  $\Omega_0 + \lambda_0 = 1$  and  $\delta_c = 1.69$ .

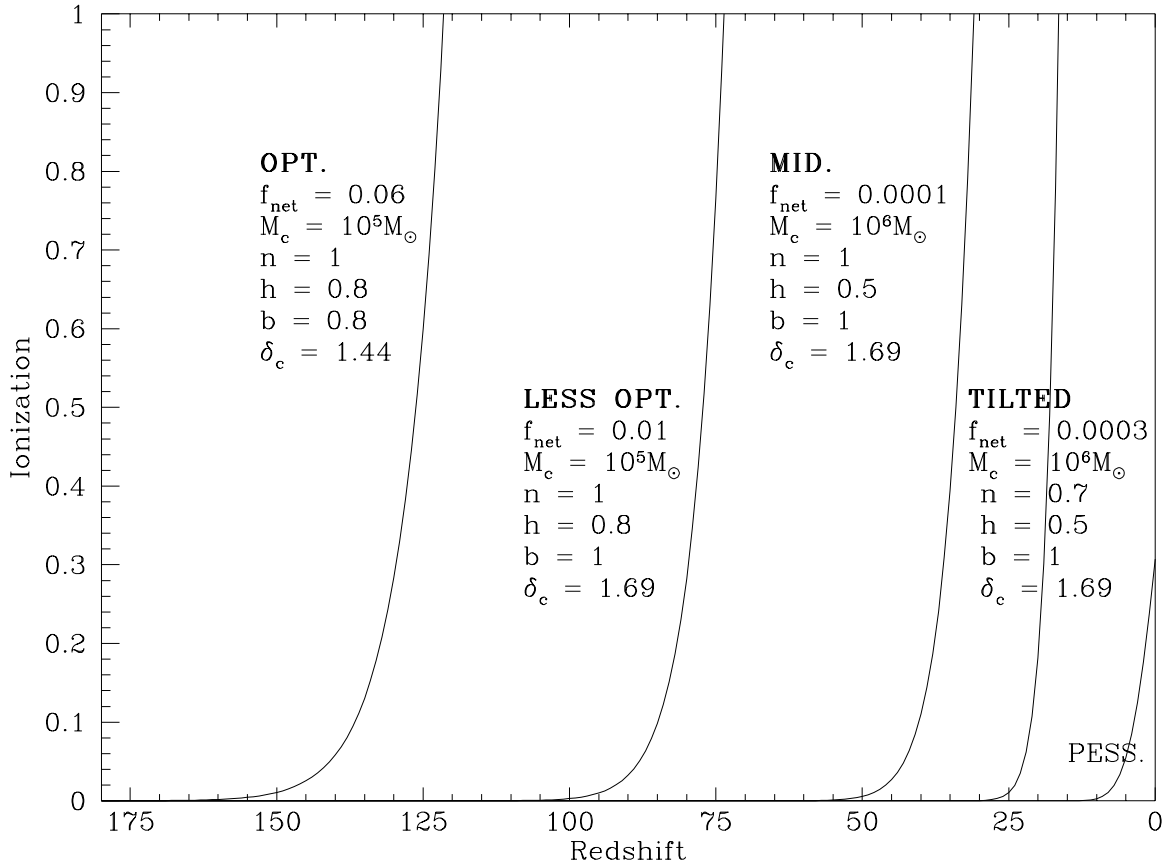


Figure 2: Volume fraction ionized for various scenarios. The volume fraction of the universe that is in ionized Strömgren bubbles is plotted as a function of redshift for various parameter choices, corresponding to  $n = 1$  CDM (optimistic, less optimistic, middle-of-the-road and pessimistic cases) and the tilted power spectrum ( $n=0.7$ ) variant of CDM.

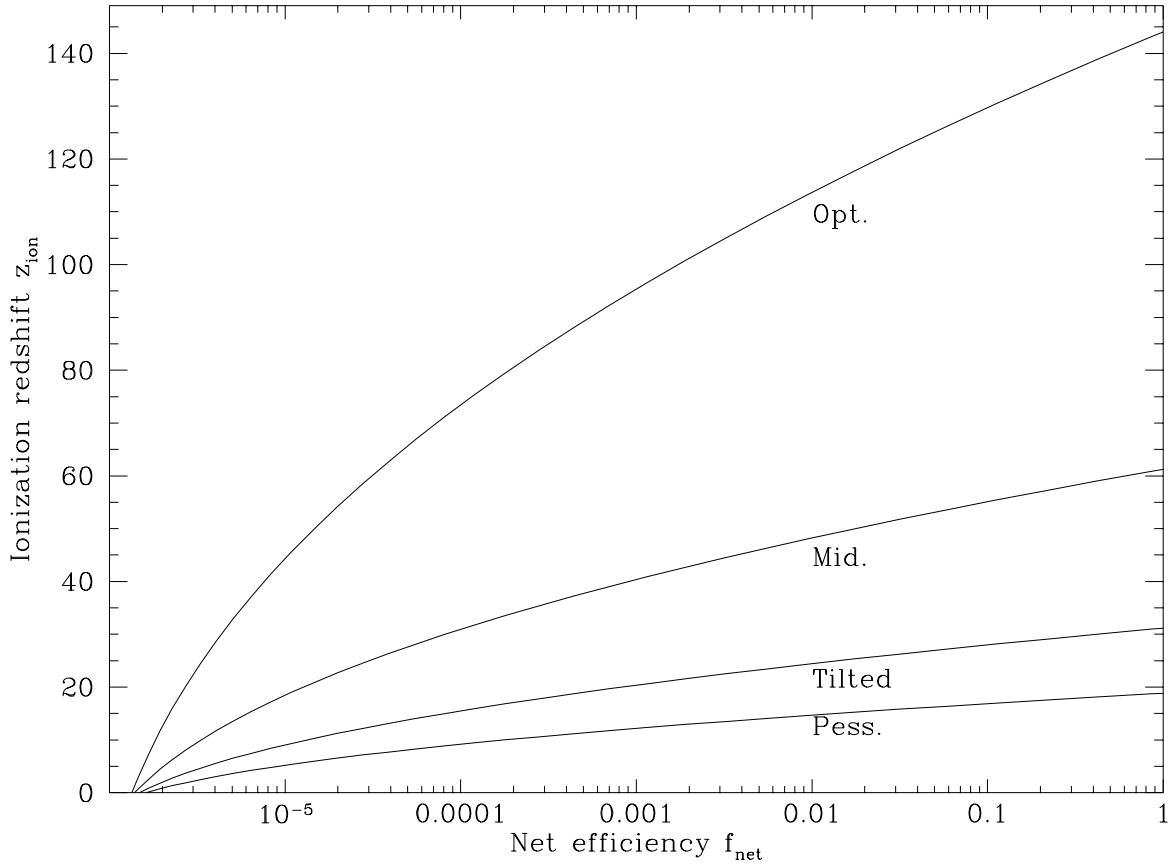


Figure 3: Ionization redshift for various scenarios. The redshift at which  $x = 0.5$  plotted as a function of the net efficiency. The four curves correspond to four of the choices of  $z_{\text{vir}}$  in Table 1: 41.4, 17.2, 8.4 and 4.8 from top to bottom.

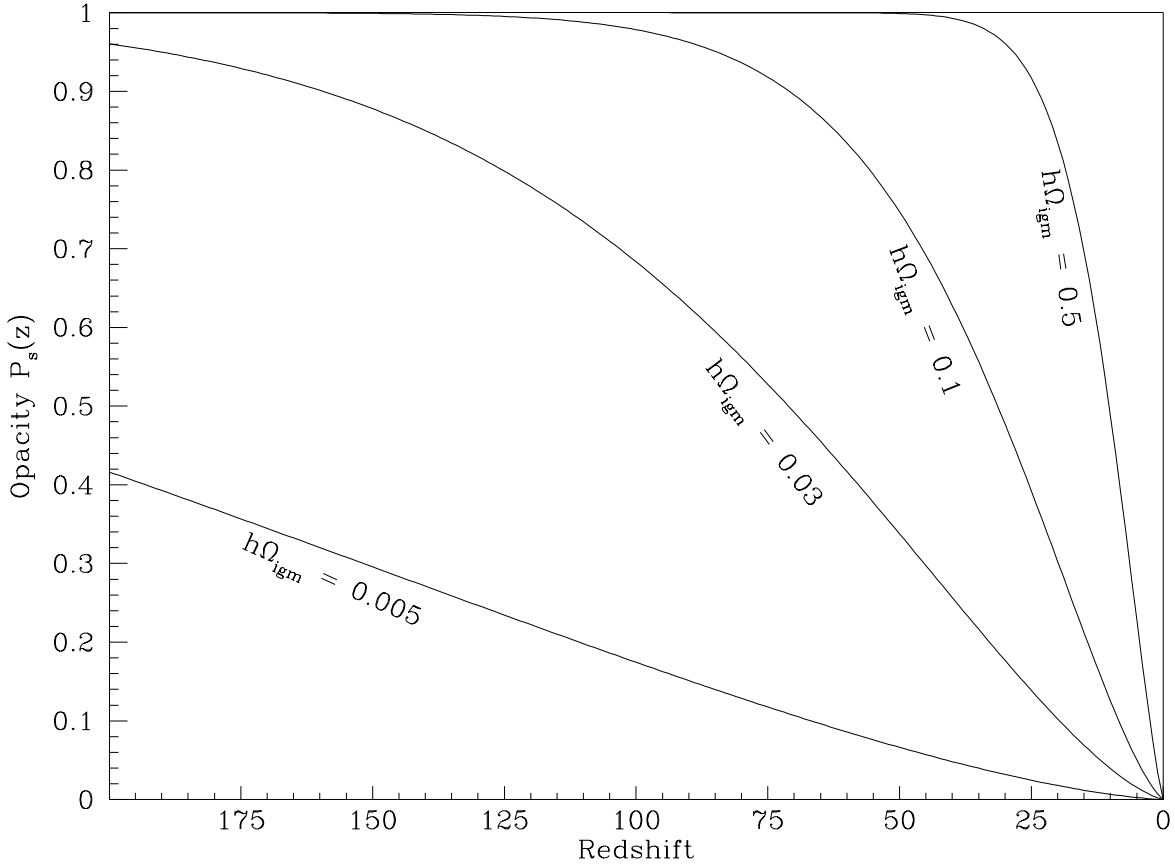


Figure 4: Opacity for completely ionized IGM.

The Thomson opacity  $P_s(z)$ , the probability that a CBR photon has been scattered at least once after the redshift  $z$ , is plotted for four different choices of  $h\Omega_b$  for the case where the IGM is completely ionized at all times. For more realistic scenarios where ionization occurs around some redshift  $z_{\text{ion}}$ , the opacity curves simply level out and stay constant for  $z \gg z_{\text{ion}}$ .

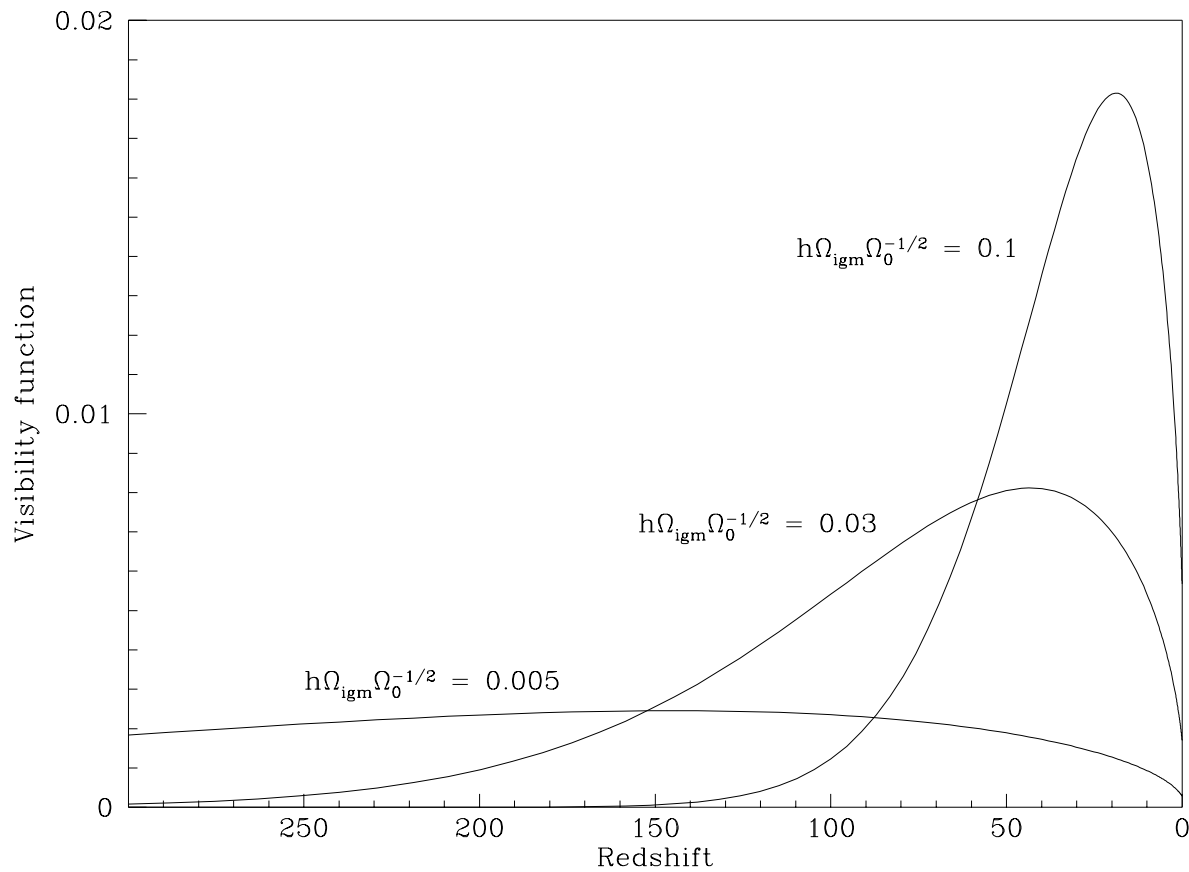


Figure 5: Last-scattering surface for completely ionized IGM. The probability distribution for the redshift at which a CBR photon was last scattered, the so called visibility function, is plotted for four different choices of  $h\Omega_b$  for the case where the IGM is completely ionized at all times. For more realistic scenarios where ionization occurs around some redshift  $z_{ion}$ , the curves are unaffected for  $z \ll z_{ion}$ , vanish for  $z_{ion} \ll z \ll 10^3$  and have a second bump around  $z \approx 10^3$ .

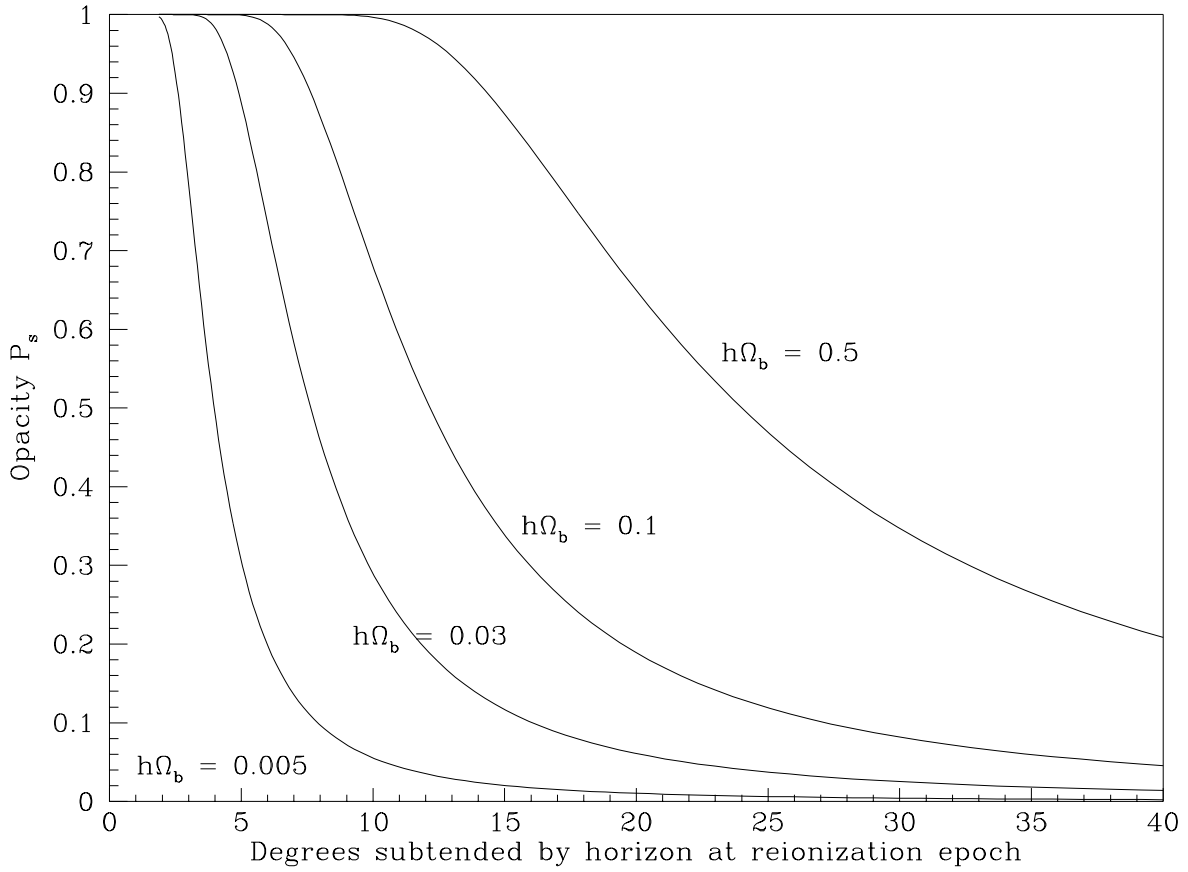


Figure 6: Opacity for completely ionized IGM as function of angle. The total Thomson opacity  $P_s$ , the probability that a CBR photon has been scattered at least once since the recombination epoch, is plotted as a function of the angle in the sky that the horizon subtended at the reionization epoch. This is the largest angular scale on which fluctuations can be suppressed.

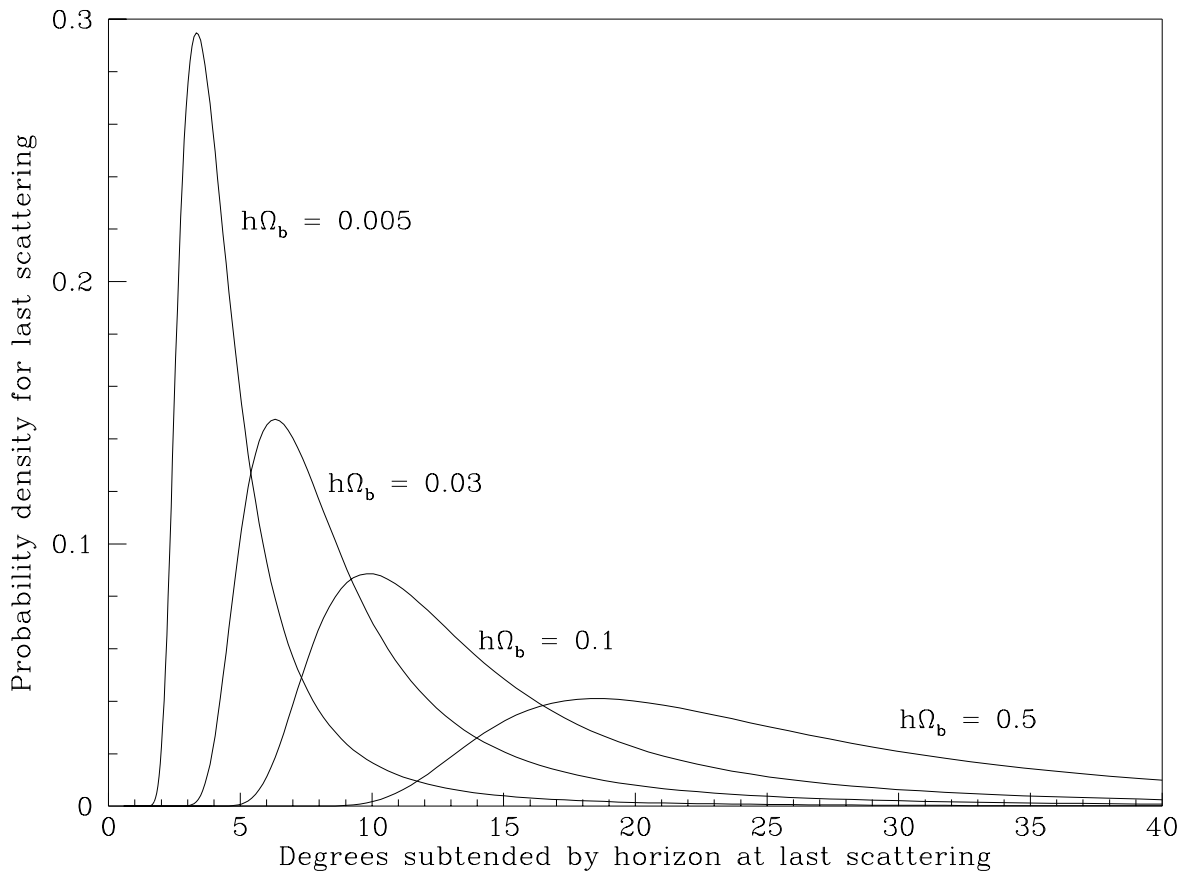


Figure 7: Last-scattering surface for completely ionized IGM as function of angle.

The probability distribution for the angle subtended by the horizon when a CBR photon was last scattered, the so angular visibility function, is plotted for four different choices of  $h\Omega_b$  for the case where the IGM is completely ionized at all times. For more realistic scenarios where ionization occurs around some redshift  $z_{ion}$ , corresponding to an angle  $\theta_{ion}$ , the curves are unaffected for  $\theta \gg \theta_{ion}$ , vanish for  $2^\circ \ll \theta \ll \theta_{ion}$  and have a second bump around  $\theta \approx 2^\circ$ , the horizon angle at recombination.

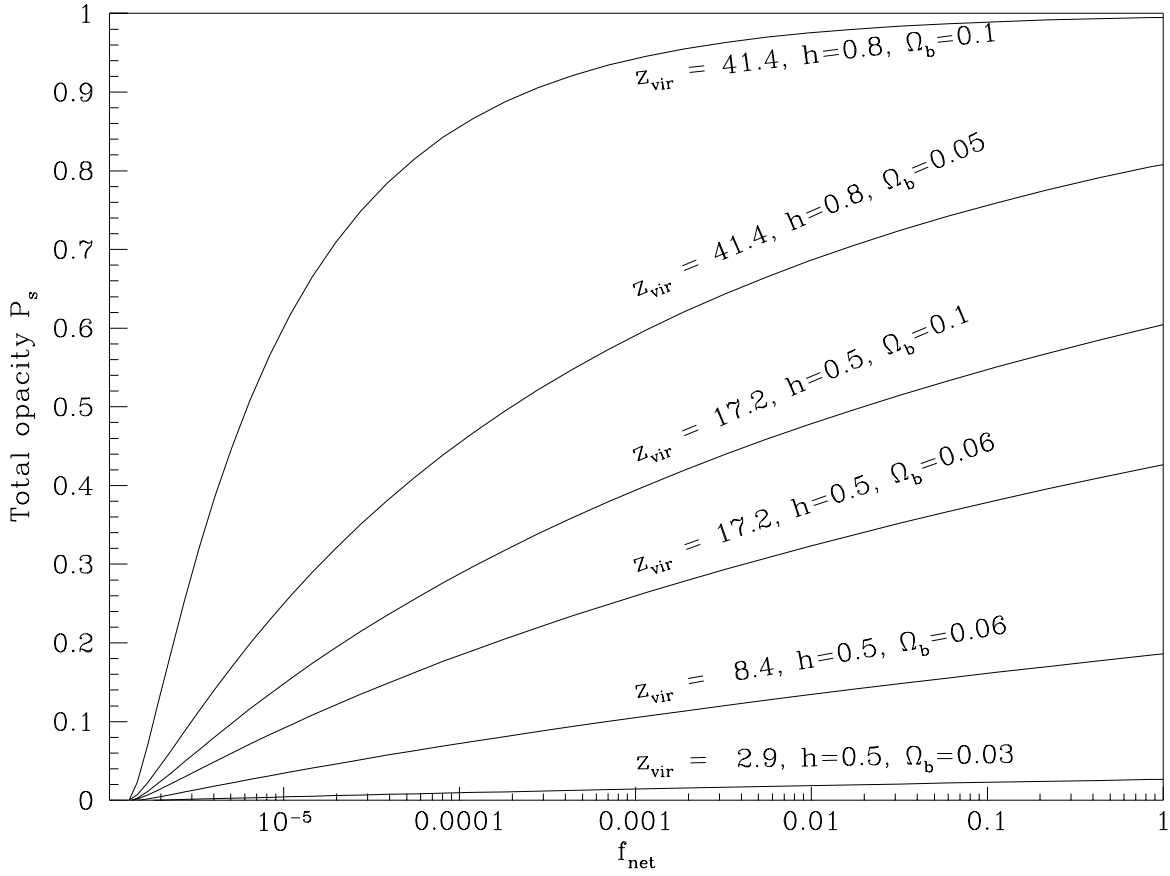


Figure 8: Total opacity for various models. The total opacity, the probability that a CBR photon has been scattered at least once since the recombination epoch, is plotted for a variety of models.

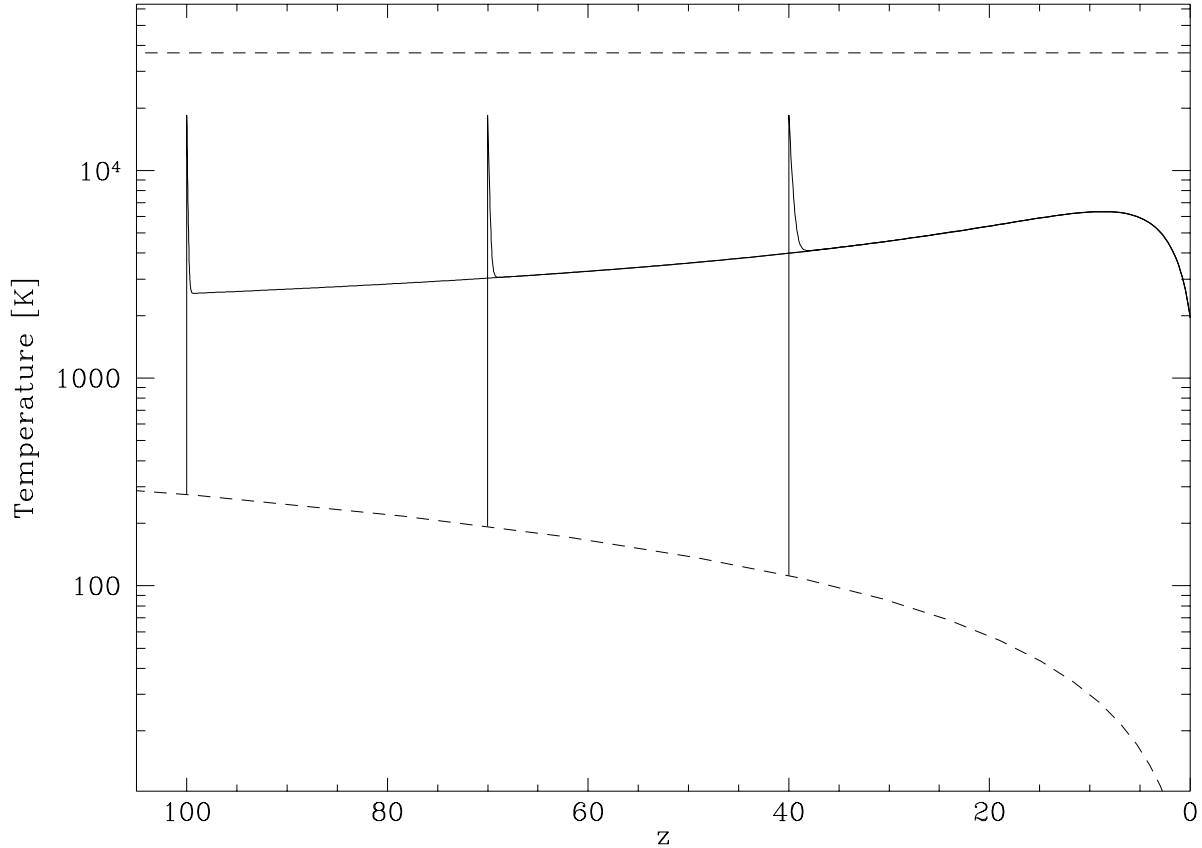


Figure 9: Temperature evolution in intergalactic Strömrgren bubbles. The temperature evolution is plotted for IGM exposed to a UV flux strong enough to keep it completely photoionized. In this example,  $h = 0.5$ ,  $\Omega_b = 0.06$ , and  $T^* = 36,900$ . The upper dashed line is  $T^*$ , the temperature corresponding to the average energy of the released photoelectrons, towards which the plasma is driven by recombinations followed by new photoionizations. The lower dashed line is the temperature of the CBR photons, towards which the plasma is driven Compton cooling. The three solid curves from left to right correspond to three different redshifts for becoming part of a Strömrgren bubble. The first time the hydrogen becomes ionized, its temperature rises impulsively to  $T^*/2$ . After this, Compton cooling rapidly pushes the temperature down to a quasi-equilibrium level, where the Compton cooling rate equals the recombination heating rate.

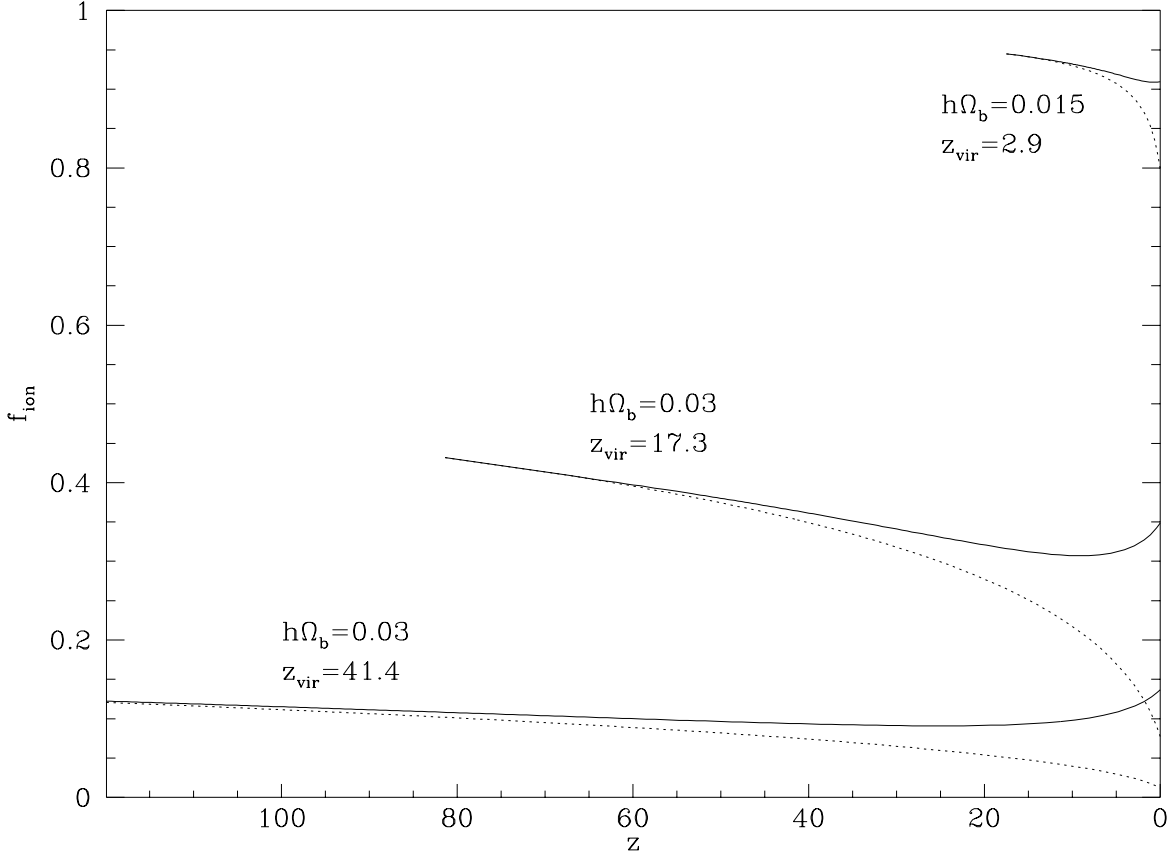


Figure 10: Ionization efficiencies for various scenarios.

The ionization efficiency, the fraction of the UV photons that produce a net ionization, is plotted for three different parameter combinations. In all cases,  $T^* = 36,900\text{K}$ , the value appropriate for the radiation from the population 3 star in Table 3. The solid lines are the exact results from numerical integration of equation (13). The dotted lines are the analytic fits, which are seen to agree well in the redshift range of interest, which is typically  $z$  twice or three times  $z_{\text{vir}}$ .